Size Statistics of Cumulus Cloud Populations in Large-Eddy Simulations.

R. A. J. NEGGERS*
Royal Netherlands Meteorological Institute, De Bilt, the Netherlands

H. J. J. JONKER
Delft University of Technology, Delft, the Netherlands

A. P. SIEBESMA
Royal Netherlands Meteorological Institute, De Bilt, the Netherlands

1. Introduction

Shallow cumulus cloud fields are inhomogeneous and broken in structure, and the individual clouds are irregular over a wide range of scales. This complicates the parameterization of the radiative and transport effects of such cloud ensembles in General Circulation Models (GCMs) (e.g. Arakawa and Schubert 1974; Tiedtke 1989). This has been the motivation behind many observational studies of shallow cumulus cloud populations. Such studies have used aircraft photographic images, radar data, satellite images and other remote sensing instruments. The functional form that best describes the *cloud size distribution* is still a matter of debate (Plank 1969; Wielicki and Welch 1986; Lopez 1977; Cahalan and Joseph 1989; Kuo et al. 1993; Benner and Curry 1998).

Concerning the cloud fraction, small cumulus clouds are the most numerous in the population but cover a relatively little area individually. On the other hand, large clouds individually cover a large area but occur relatively seldom. Due to this trade-off between cloud number and cloud size, it is not known a priori what is the size of the clouds which contribute most to the total cloud fraction of the population. Observational evidence was presented by Plank (1969) and by Wielicki and Welch (1986), which showed that an intermediate size between the largest and smallest size present in the population dominated the cloud fraction. The dominating size varies over the cumulus scenes studied, but is always well-defined and intermediate.

In this study, *cloud size distributions* of shallow cumulus cloud populations are calculated using Large-Eddy Simulation (LES). Our aim is to critically compare LES results to the high-resolution observations of real cloud populations, in order to evaluate the representativeness of cloud populations as produced by LES. To enable a straightforward comparison, the same algorithm is applied as in observational studies using high-altitude photography or remote sensing, and a comparable number of clouds is sampled. The universality of the cloud size distributions obtained from LES is assessed by searching for relevant scales in a range of simulated different shallow cumulus cases.

* *Corresponding author address:* R. A. J. Neggers, Royal Netherlands Meteorological Institute, P.O.Box 201 3730 AE De Bilt, the Netherlands. E-mail: neggers@knmi.nl

2. The LES model and case descriptions

A detailed description of the KNMI LES model used in this study is given by Cuijpers and Duynkerke (1993). Three different shallow cumulus cases are selected for simulation, in order to assess the universality of the resulting cloud size distributions. Each LES case is based on the measurements and observations made during the measurement-campaign of the corresponding name. The first case is based on the Barbados Oceanographic and Meteorological Experiment (BOMEX) during which marine steady state cumulus convection was observed for a period of several days Siebesma et al. (2002). The second case is based on observations on August 5, 1995 during the Small Cumulus and Microphysics Study (SCMS). On this day, strong cumulus convection was observed over land (Neggers et al. 2002b), with a significantly larger surface fluxes compared to BOMEX. The third case is based on development of shallow cumulus over land such as observed on June 21st, 1997 at the Southern Great Plains (SGP) site in Oklahoma of the Atmospheric Radiative Measurement (ARM) program (Brown et al. 2001).

Several runs were performed of each case, each with a differently randomnized initial temperature profile in order to obtain as many statistically independent clouds for the calculation of the cloud size distributions. This resulted in approximately $4 \cdot 10^4$ sampled clouds in each case, which makes the statistical quality of the resulting histograms comparable to the observational studies mentioned above.

3. The method

The *cloud size distributions* of a cumulus cloud population is defined as the integral over a probability density function (pdf). This pdf, also known as a *cloud size density*, is the probability of occurence of a cloud of a certain size. Cloud size *decompositions* can be calculated for some important properties which characterize the population, i.e. the cloud fraction and the vertical mass flux as a function of cloud size.

Each cloud n in the population is first given a unique linear size ℓ_n, defined as the square root of its vertically projected area A_n^p,

$$\ell_n = \sqrt{A_n^p} \tag{1}$$

Next all the clouds are sorted by their size which results in histograms. This algorithm is described in full detail by Neggers et al. (2002a). The total number of clouds N present in the domain at a certain time is defined by the integral of the corresponding cloud size density $\mathcal{N}(l)$:

$$N \equiv \int_0^\infty \mathcal{N}(l) dl, \tag{2}$$

where the term $\mathcal{N}(l)$ is the number of clouds of size l in the domain. The vertical projected cloud fraction a^p of a cloud field is defined as the ratio between the vertically projected area covered by all clouds and the total area of the domain. The *cloud fraction decomposition* α^p is then defined by

$$a^p \equiv \int_0^\infty \alpha^p(l) dl, \quad \alpha^p(l) \equiv \frac{l^2\, \mathcal{N}(l)}{L_x L_y}, \tag{3}$$

where L_x and L_y are the horizontal dimensions of the domain. This means that once $\mathcal{N}$ is known α^p is also known. Finally, the *mass flux decomposition* $\mu(l)$ is defined as the height-averaged mass-flux of all clouds of size l,

$$m \equiv \int_0^\infty \mu(l) dl, \tag{4}$$

where m is the total mass flux.

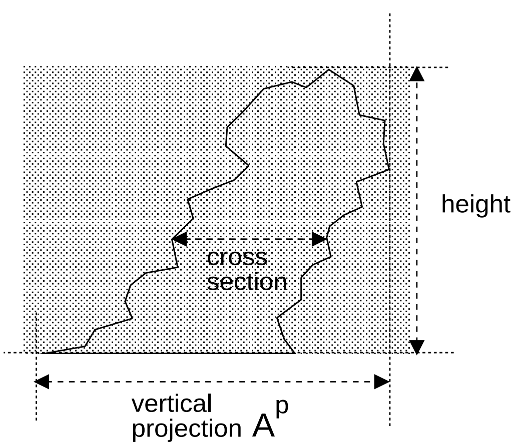

FIGURE 1: Several different measures of a single cumulus cloud, shown in a schematic vertical cross-section.

4. Objectives

The ultimate goal is to find out if a universal functional form exists for the cloud size density that contains a minimum but enough non-universal parameters to apply to all situations. However, there is no agreement on the this yet. For example, several possible candidates are mentioned in the literature to describe the decreasing cloud size density $\mathcal{N}$ as observed in natural cloud populations. The most frequently mentioned proposition in recent years is the power-law (Cahalan and Joseph 1989; Kuo et al. 1993; Benner and Curry 1998),

$$\mathcal{N}(l) = a\, l^b. \tag{5}$$

A scale break is defined as the cloud size at which this functional relation breaks down (the size where the power b suddenly changes). Many scale-breaks have been reported in observational studies, always at a different cloud size, and it is not yet known which physical process controls its position.

The cloud size densities $\mathcal{N}(l)$ obtained with LES in this study are also fitted with power-laws, as the corresponding parameters of this functional form are available in the literature for many real cloud fields. The agreement between the observed and simulated the power-law exponents is an indication of how realistic the simulated cloud populations actually are. These results are then used to examine the universality of the functional form thought to be applicable to the cloud size density. To this purpose some the size densities from the three different cumulus regimes are scaled with relevant parameters, in order to reduce the problem of reconstructing the cloud size density to a minimum number of parameters. Finally the underlying relations between the cloud size density and the decompositions of cloud fraction and mass flux are used to explain the typical shape of these size decompositions.

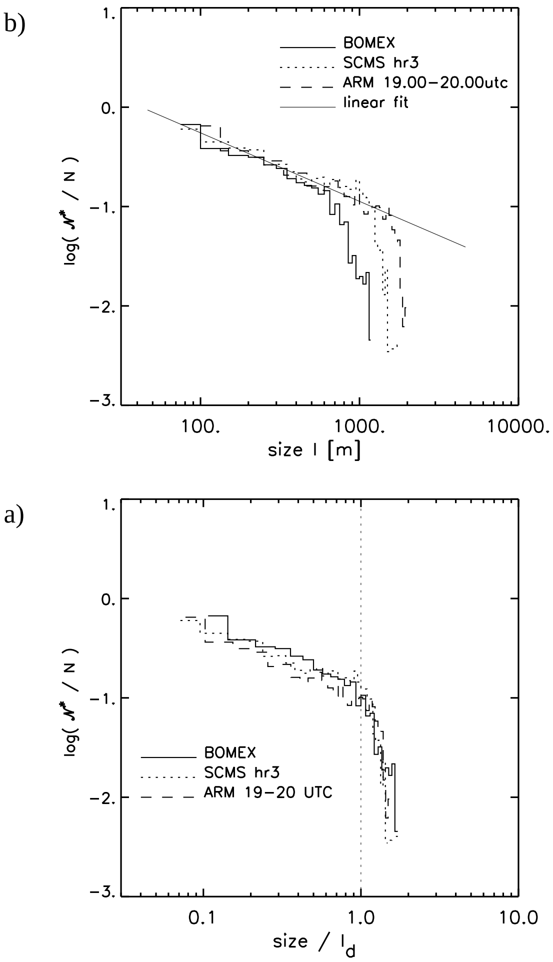

FIGURE 2: The normalized cloud size density $\mathcal{N}^*$/N of a) the BOMEX, SCMS and ARM cases. The solid line corresponds to the linear fit $\mathcal{N}^*/\mathrm{N} = 1.121 - 0.70 \log l$, based on the points with cloud sizes smaller than the scale-break size. Panel b) shows the same densities with the cloud size divided by their scale-break size.

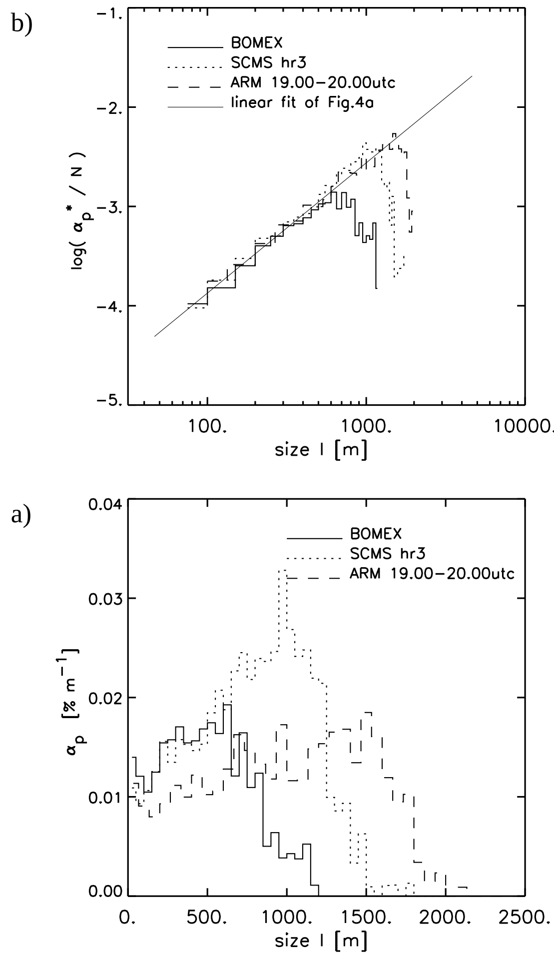

FIGURE 3: The normalized projected cloud fraction decomposition $\alpha^{p\,*}$/N of a) the BOMEX, SCMS and ARM cases. The linear fit corresponding to Figure 2a using (3) is also plotted as a solid line.

5. Results

The cloud size densities of the simulated cloud populations are described well by a power-law at the smaller sizes in all cases, see Figure 2a. This scaling covers roughly one decade of cloud sizes, with a power-law exponent of -1.70 which is comparable to observations (Cahalan and Joseph 1989; Benner and Curry 1998). Apparently this power-law decay of the cloud size density is a robust feature in LES. In all cases the scaling area is bounded by a scale-break, above which number of clouds decreases more rapidly with size l.

These results suggest that the powerlaw-exponent is case-independent, and that scale-break size is the only relevant variable scale. Therefore we further scale the cloud size densities by non-dimensionalizing the cloud size with the scale-break size (see Fig. 2b). The data-collapse in this figure of all cases over all sizes corroborates the idea of a universal description of the whole cloud size density, also above the scale break. In this region clearly another exponent applies, or perhaps even a totally different functional form. Nevertheless, Fig.2b illustrates that the scale-break size is the only variable.

The projected cloud fraction decomposition α^p is uniquely determined by the number density $\mathcal{N}$, see (3). Figure 3a indicates that the intermediate maximum in α^p is located at the position of the scale-break in $\mathcal{N}$. Figure 3b shows α^p non-normalized on linear axes (a common format in many presentations of observational results). The total projected cloud fraction a^p in each case is the surface covered by the histogram. The fact that the dominating size in α^p is intermediate results from the existence of the scale-break in $\mathcal{N}$. In accordance with obser-

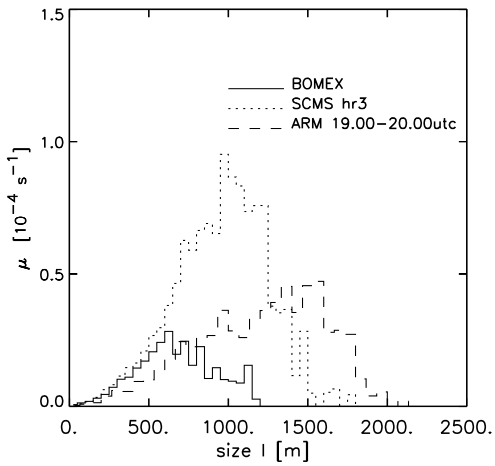

FIGURE 4: Cloud size decompositions of the BOMEX, SCMS and ARM case of the vertical mass flux μ.

vations we do find a scale-break in LES, with $b = -1.70$ below and $b < -2$ above the scale-break size. Because $\alpha^p(l) \sim l^{(b+2)}$ via (3) this implies that $\alpha^p(l)$ increases with l below the scale-break and decreases above it, and hence a dominating size which is intermediate. This shows that the existence of the scale-break in $\mathcal{N}$ is essential for the presence of an intermediate dominating size in α^p. Knowledge of the position of the scale-break directly gives the dominating size in the projected cloud fraction and vice versa.

In the mass-flux decomposition μ(l) as shown in Fig.4 the dominating size is even better defined, although shifted somewhat towards the larger sizes compared to the projected cloud fraction decomposition. The smallest clouds in the spectrum contribute close to nothing to the vertical transport, mainly because of their very low vertical velocities.

6. Discussion and Conclusions

These results show that the cloud size distributions produced by LES resemble those of real cloud populations on several important points, such as the powerlaw exponent of -1.70 and the presence of a scale break. The cloud size densities show a remarkable uniformity over the three simulated cases, the only variant being the position of the scale-break, and with it the intermediate dominating size in the cloud fraction. This feature facilitates the parameterization of these densities. Which process actually sets the scale-break size remains unclear and is not answered in this study. The LES concept would be a suitable numerical laboratory to further investigate this phenomenon (e.g. Jonker et al. 1999).

The intermediate position of the dominating cloud size shows that the clouds which are most important for the projected cloud fraction and vertical transport are not of resolution-scale but are significantly larger. This is convenient, for the sub-grid model of LES plays an important role in the dynamics of the smallest clouds, while the larger clouds are resolved better by the discretized governing equations. We find here that those larger, better-resolved clouds contribute most to the total projected cloud fraction and mass flux of the population. The smallest clouds contribute close to nothing to the vertical mass transport.

REFERENCES

Arakawa, A., and W. H. Schubert, 1974: Interaction of a cumulus cloud ensemble with the large-scale environment, part I. *J. Atmos. Sci.*, **31**, 674-701.

Benner, T. C., and J. A. Curry, 1998: Characteristics of small tropical cumulus clouds and their impact on the environment. *J. Geoph. Res.*, **103**, 28753-28767.

Brown, A. R., 1999b: The sensitivity of large-eddy simulations of shallow cumulus convection to resolution and sub-grid model. *Q. J. R. Met. Soc.*, **125**, 469-482.

Brown, A. R., A. Chlond, C. Golaz, M. Khairoutdinov, D. C. Lewellen, A. P. Lock, M. K. MacVean, C-H. Moeng, R. A. J. Neggers, A. P. Siebesma and B. Stevens: Large-eddy simulation of the diurnal cycle of shallow cumulus convection over land. *Accepted for publication in the Q. J. R. Met. Soc.*.

Cahalan, R. F., and J. H. Joseph, 1989: Fractal statistics of cloud fields. *Mon. Wea. Rev.*, **117**, 261-272.

Cuijpers, J. W. M., and P. G. Duynkerke, 1993: Large-eddy simulation of trade-wind cumulus clouds. *J. Atmos. Sci.*, **50**, 3894-3908.

Jonker, H. J. J., A. P. Siebesma and P. G. Duynkerke, 1999: Development of mesoscale fluctuations in cloud-topped boundary layers. Proceedings of the 13th symposium on boundary layers and turbulence, Dallas, USA. American Meteorological Society, 45 Beacon Street, Boston Massachusetts, MA02108-3693, USA.

Lopez, R. E., 1977: The lognormal distribution and cumulus cloud populations. *Mon. Wea. Rev.*, **105**, 865-872.

Kuo, K. -S., R. M. Welch, R. C. Weger, M. A. Engelstad, and S. K. Sengupta, 1993: The three-dimensional structure of cumulus clouds over the ocean, I, Structural analysis. *J. Geoph. Res.*, **98**, 20685-20711.

Neggers, R. A. J., H. J. J. Jonker and A. P. Siebesma. Size statistics of cumulus cloud populations in large-eddy simulation. *Accepted for publication in the J. Atmos. Sci.*

Neggers, R. A. J., P. G. Duynkerke and S. M. A. Rodts. Shallow cumulus convection: a validation of large-eddy simulation against aircraft and Landsat observations. *Submitted to the Q. J. R. Met. Soc.*

Plank, V. G., 1969: The size distributions of cumulus clouds in representative Florida populations. *J. App. Met.*, **8**, 46-67.

Siebesma, A. P., C. S. Bretherton, A. Brown, A. Chlond, J. Cuxart, P. G. Duynkerke, H. Jiang, M. Khairoutdinov, D. Lewellen, C.-H. Moeng, B. Stevens and D. E. Stevens: An intercomparison study for cloud resolving models of shallow cumulus convection.*Submitted to J. Atmos. Sci.*

Stevens, B., A. S. Ackerman, B. A. Albrecht, A. R. Brown, A. Chlond, J. Cuxart, P. G. Duynkerke, D. C. Lewellen, M. K. MacVean, R. A. J. Neggers, E. Sanchez, A. P. Siebsema, D. E. Stevens, 2001: Simulations of trade-wind cumuli under a strong inversion. *J. Atmos. Sci.*, **58**, 1870-1891.

Tiedtke, M., 1989: A comprehensive mass flux scheme for cumulus parameterization in large-scale models. *Mon. Wea. Rev.*, **177**, 1779-1800.

Wielicki, B. A., and R. M. Welch, 1986: Cumulus cloud properties derived using landsat satellite data. *J. Clim. and Appl. Meteorol.*, **25**, 261-276.